Id.: CR09

Evaluation of Dose Profiles for Small Fields in 10 MV Beam Radiotherapy using Solid Water Phantom

Caio Fernando Teixeira Portela[1], André Ezequiel Lôbo de Abreu[1,2], Stephanie dos Santos[1], Arnaldo Prata Mourão[1], Adriana de Souza Medeiros Batista[1,3]

[1]Departamento de Engenharia Nuclear, Escola de Engenharia, UFMG
Avenida Antônio Carlos, 6627, Pampulha
[2]Rede MaterDei de Saúde, Serviço de Radioterapia, Unidade Santo Agostinho
Rua Gonçalves Dias, 2700, Santo Agostinho
[3]Departamento de Anatomia e Imagem, Faculdade de Medicina, UFMG
Avenida Antônio Carlos, 6627, Pampulha

caiofernando_fisica@yahoo.com.br

Palavras-Chave: Radiotherapy; Small Fields; Radiochromic Film
Área: Ciências das Radiações
Sub-área: Aplicações das Radiações à Biomédica

ABSTRACT

Radiation therapy is a crucial technique in the treatment of cancers, often combined with other therapeutic approaches such as chemotherapy and immunotherapy. Radiotherapy uses linear accelerators to perform treatment using electron beams and X-ray photons, aiming to destroy or prevent the proliferation of tumor cells. Technologies for radiotherapeutic treatment have advanced rapidly, necessitating more dynamic planning for different patients. Advances in stereotactic radiosurgery (SRS), stereotactic body radiotherapy (SBRT) for both cranial and extracranial lesions, intensity-modulated radiation therapy (IMRT), and volumetric modulated arc therapy (VMAT) use relatively small fields, smaller than 4x4 cm². Dosimetric analysis for X-ray beams in radiotherapy for small fields presents difficulties due to electronic disequilibrium, source occlusion, high dose gradients, and the average volume of detectors. However, dosimetric analysis for these fields faces challenges due to electronic imbalance, source obstruction, high dose gradients, and reduced detector size. These facts demonstrate the importance of determining and acquiring dosimetric data, understanding the appropriate detectors to be used in each situation, and evaluating the computerized planning system. Errors in planning calculations resulted in higher than planned doses for patients, highlighting the importance of accurate determination of dosimetric data, proper selection of detectors, and rigorous evaluation of computerized planning systems. This work conducts a dosimetric analysis in small fields of the VersaHD accelerator from the manufacturer Elekta, using Gafchromic EBT3 radiochromic films, with the use of a solid water phantom to survey dose variations in different field sizes. Irradiations refer to axial and longitudinal fields ranging from 1x1 to 10x10 cm². The results revealed significant variations in dose deposition as a function of field size and among the equipment evaluated.

1. INTRODUÇÃO

The National Cancer Institute (INCA), in a document published in 2023, indicated that it expects 704 thousand new cases of cancer in Brazil for each year of the 2023-2025 triennium. Cancer is the second leading cause of death in Brazil, second only to cardiovascular diseases. Among the prevention, control and treatment actions is radiotherapy. Radiotherapy is a treatment whose working principle is the ability to concentrate the deposition of dose on tumor cells and seek to spare neighboring healthy tissues. Radiotherapy is constantly evolving, with technological and scientific advances that allow further improving treatment results, to contribute to the reduction of tumor size, local control of the disease and improvement of patient survival. The decision to use radiotherapy as part of the treatment plan is made considering the stage of the disease, the location of the tumor, the patient's clinical conditions, and the therapeutic goals [1-4].

Conventional radiotherapy treatment fields use dimensions close to 10x10 cm², varying according to the treatment. However, with the advancement and increasing use of radiotherapy techniques, for treatments in intensity-modulated radiotherapy (IMRT), volumetric modulated arc therapy (VMAT), stereotactic radiosurgery (SRS), stereotactic radiotherapy (SRT) and body radiotherapy (SBRT), as well as in units of cobalt-60 and small fields. These radiotherapy treatment techniques use small irradiation fields, smaller than 4x4 cm², a size that has been described in the literature as a field affected by electronic imbalance. The evolution of the radiotherapy techniques and protocols available for the treatment of cancer have introduced new theoretical and practical standards to ensure the quality and reliability of these techniques. IMRT is a technique that uses tomographic images during the physical planning of cancer patient treatment. This type of treatment modulates the number of photons that cross a given area, modifying the beam's intensity conforming the dose to the target volume that aims to maximize the radioprotection of surrounding tissues [5-8].

Small fields are being applied in radiotherapy, include IMRT, VMAT, SRS, SRT and SBRT. The small fields are produced by the implementation of collimation tools through Cones and Multileaf Collimators (MLC) or by devices dedicated to this purpose, such as Cyberknifes and Gamma Knives. The influencing factors include finite source size, steep dose gradients, charged particle disequilibrium, detector size and associated volume averaging effects, and changes in energy spectrum and associated dosimetric parameters. Conventionally, external-beam machines like linear accelerators with jaws or MLCs are able to produces fields of typical dimensions smaller than 4×4 cm² when being used to deliver therapeutic dose to cancer patients. A small field is understood like a field created by downstream collimation of a flattened or unflatten photon beam and differ from conventional fields in their lateral dimensions, causing penumbra areas on both sides of the field to overlap and make most commonly used detectors large in relation to the size of the radiation field. The technological development in radiotherapy, the use of increasingly smaller and/or modulated small fields generated an increase in the uncertainty of the acquisition of dosimetric data. In the literature, incidents caused by errors in the acquisition of these data from the treatment machine related to small fields have been reported [9-12].

In this work, the dose distribution of an X-ray beam was recorded using a solid water phantom. This phantom was irradiated using small fields with 1x1, 2x2, 3x3 and 5x5 cm². The 10 MV X-ray beam was generated in a linear accelerator model Synergy Platform from the manufacturer Elekta, and radiochromic film sheets were used to record dose profiles inside a solid water phantom.

2. MATERIALS AND METHODOLOGY

2.1 Linear Accelerator

The linear particle accelerator is a Versa HD model, from the manufacturer Elekta, which allows the generation of photon beams generated at voltages of 6 MV and 10 MV. The field size at the isocenter ranges from 1x1 to 40x40 cm², the leakage radiation from the head is less than 0.1% of the dose rate at the isocenter. The accelerator is equipped with an Agility multileaf collimator (MLC), consisting of 160 blades with a thickness of 5.0 mm that form the irradiation fields and to verify the positioning of the blades the Rubicon optical system is used. Figure 1 shows a frontal image of the VersaHD linear accelerator, in which the head above and the patient positioning table below are seen in the foreground [13-14].

Fig. 1. Linear Accelerator Elekta VersaHD

2.2 Solid Water Phantom

The solid water simulator used in the calibration curve survey was built with solid water slides. Two 30x30x1 cm³ plates and one 30x30x2 cm³ complementary plate were used. These plates respond to radiation beams in a similar way to water, with an error of 1% and aid in the search for data on dose distribution as it approximates the radiation absorption and scattering properties of muscles and other soft tissues. This material allows for better handling as it is solid and widely used in the manufacture of human simulator objects and the phantom allows to place radiation detectors in a solid material and can substitute the water. Another reason for the choice is because it is universally available as reproducible material for radiation properties [15-16].
The Figure 2 presents a frontal image of the solid water phantom.

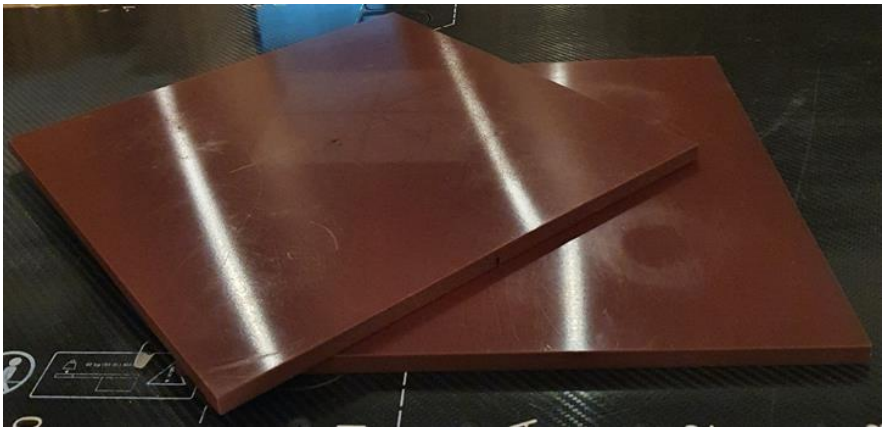

Fig. 2. Solid Water Phantom

2.3 RADIOCHROMIC FILM EBT3

The Gafchromic Radiochromic Film, model EBT3, used in the experiments has construction characteristics like other models of radiochromic films, being a tool for a wide range of doses, equivalent to soft tissues, and can be handled in light rooms. EBT dosimetry film is made by laminating a sensitive layer between two layers of polyester and it is used for measurements of absorbed doses of 3.0 Gy, making it more suitable for applications in radiotherapy and radiosurgeries. Radiochromic films when exposed to radiation show a darkening proportional to the dose received. As higher is the absorbed dose, as darker they become. The technical features of Gafchromic EBT3 include suited for applications such as IMRT and VMAT and enables non-uniformity correction by using multi-channel dosimetry [14]. The Figure 3 shows images of a 7x7 cm^2 strip, before (a) and after irradiation with a field aperture of 5x5 cm^2 (b). After separating the color channels, images of the red channel, in grayscale, were obtained before exposure and after [17-21].

After separating the color channels, images of the red channel, in grayscale, were obtained before exposure and after. The information contained in the non-irradiated strip was used to reference the background value (BG). The color digital images were generated in the G4050 photographic scanner, in reflective mode, with a resolution of 300 ppi, in TIFF format. These images, in RGB, were worked on in the ImageJ software, which was used to separate the color channels, obtaining the images in grayscale of each of the colors, red, green, and blue.

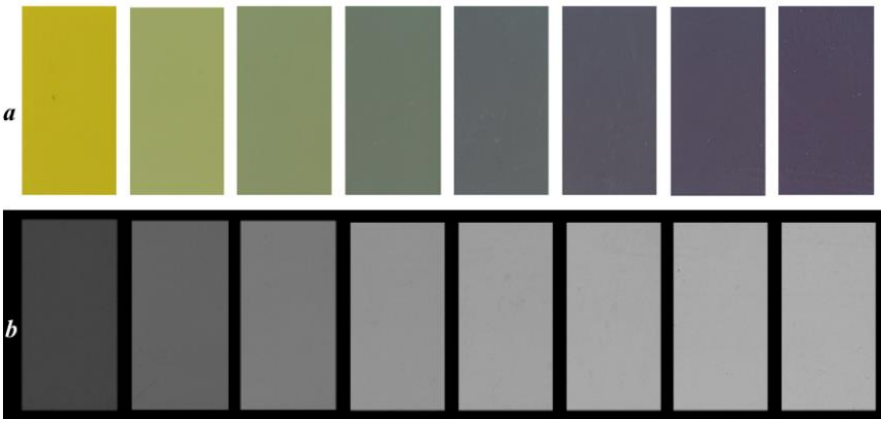

Fig. 3. Images of the strip of the EBT3 film. Before exposure (a), after exposure (b), red channel

2.4 RADIOCHROMIC FILM RECORDS

To record the dose profiles, the phantom loaded with the radiochromic film was positioned in two different positions, in order to obtain the axial and longitudinal dose profiles, for each field size, when the phantom was irradiated with the photon beam. In the assembly to obtain the longitudinal dose profiles, the film sheet was positioned between the two plates of solid water, close to the beam incidence surface and the phantom loaded with the film sheet was irradiated laterally. In the irradiation to obtain the axial dose profiles, the film sheet was positioned inside the plates, in the center of the solid water phantom at a depth of 4.0 cm, being irradiated frontally. The strips were scanned one day before the exhibition and one day after the exhibition. The Figure 4 shows the positioning of the phantom loaded for the lateral and frontal irradiation using the 10 MV X-ray beam. This film has high sensitivity to ionizing radiations with dose in 3.0 Gy X-ray beam generated from linear accelerator (LINAC).

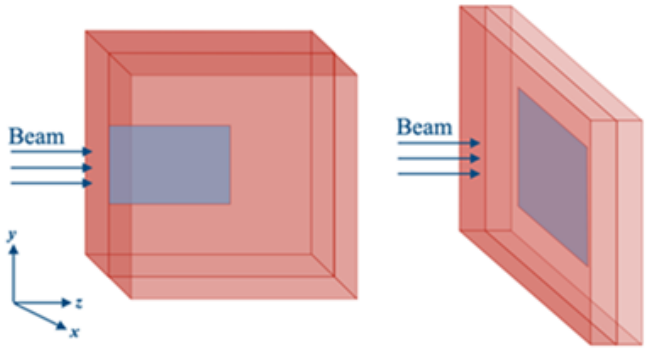

Fig. 4. The Figure presents the setup of the positioning of the film inside the solid water phantom. In a position for longitudinal irradiation that obtain de deep dose variation profile (PDD) and frontal irradiation to have the axial profiles in the axis X an Y.

The films were cut for longitudinal and axial irradiations with specific sizes for each field size. Four lateral and four frontal irradiations were performed, one each for field size. The film sheets were cut according with the field size and the photon beam incidency, in the table Table 1 have the sizes of the film sheet used.

Tab. 1. Film sheet sizes.

Field Size (cm²)	**Axial Film Size (cm²)**	**Longitudinal Film Size (cm²)**
1×1	3×3	3×15
2×2	4×4	4×15
3×3	5×5	5×15
5×5	7×7	7×15

3. RESULTS

The irradiation of the solid water phantom in 10 MV was performed with the application of 3.0 Gy in the water and the axial and longitudinal dose profile graphs were obtained with the fields of 1x1, 2x2, 3x3, 5x5, 10x10 cm² with the phantom positioned at 4.0 m from the source.

3.1 Longitudinal Dose Profile

Figure 5 illustrates the variation of the dose at depth (PDP) containing the five curves for the sizes of the 1x1, 2x2, 3x3, 5x5, 10x10 cm² fields, of the radiochromic film exposed to the X-ray beams, generated with the voltage of 10 MV. According to the graph and the values found, described in Table 2, the Depth Dose Profile (PDP), at 4.0 cm, for the 10x10 cm² field, the relative dose value is 98.35%, with little difference in relation to the 5x5 cm² field, with a dose of 97.63% at 4.0 cm. For the 1x1 cm² field, the field with the greatest effect of the electronic imbalance and the smallest irradiated field, the dose value at the reference point was 74.9%, with the maximum dose peak at the distance of 2.2 to 2.4 cm, the maximum dose peak common for all other fields.

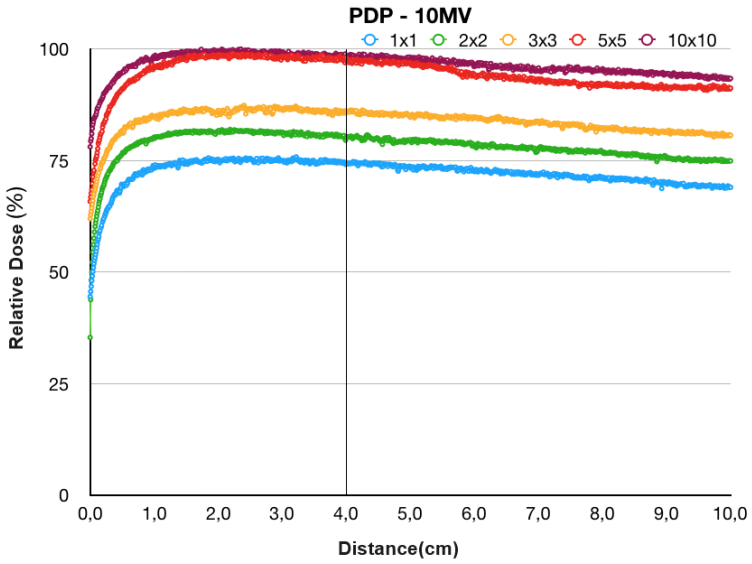

Fig. 5. The Figure presents the depth dose variation for the 10 MV beam of the film inside the solid water phantom.

For the 3x3 cm² field, followed by the 2x2 cm² and 1x1 cm² fields, the maximum relative dose was reduced due to the smaller size of the field, in which there is a gradual increase in the disturbance in the dosimetric behavior, which results in significant interference in the delivery of doses to the target volume. With this, having in hand the relative dose for each field, the size

of the field to be used in the radiotherapy treatment is defined. In the 5x5 and 10x10 cm² fields, 100% of the dose is achieved at the dose depth at 4.0 cm and for the other fields, even with a higher beam energy at an electrical voltage of 10 MV, the highest dose achieved is in the 3x3 cm² field, followed by the 2x2 and 1x1 fields. At the measured distance of 4.0 cm, for a field of 3x3 cm², the relative dose is 85.87%. For irradiation at 10 MV, the Monitor Units Used do not compensate for the drop in the curve in the Depth Dose Profiles.

Tab. 2. Results in PDP Irradiation Fields in 10 MV.

Field Size (cm²)	**Maximum Relative Dose (%)**	**Dose Relative to 4 cm (%)**	**Peak (cm)**
1x1	75,83	74,39	2,31±0,22
2x2	82,00	80,24	2,23±0,18
3x3	83,00	85,87	2,40±0,05
5x5	99,05	97,63	2,26±0,05
10x10	100	98,35	2,31±0,13

3.2 Axial Dose Profile

Figure 6a (Axis Y) and 6b (Axis X) shows the axial dose variation curves on the X and Y axes, for radiochromic film strips exposed to X-ray beams generated with a voltage of 10 MV, for the size fields of 1x1, 2x2, 3x3 and 5x5 cm². The fields on the Y axis have less distortion for the beam energy at 10 MV, when in the same accelerator used in relation to the voltage of 6.0 MV, but it is seen that for more energetic beams, the 5x5 cm² field has a greater difference in relation to the other fields presented and carried out in the experiment. The axial dose variation curves, on the X and Y axes, for the smallest irradiated field, the 1x1 cm² field, the effect of the electronic imbalance of the small fields is very evident and the distortion due to the flattening filter occurs for the 5x5 and 3x3 cm² fields, with a greater dose range for the former. At a higher energy of the irradiated photons, the relative dose in a smaller field of 1x1 cm² suffers a greater dose reduction.

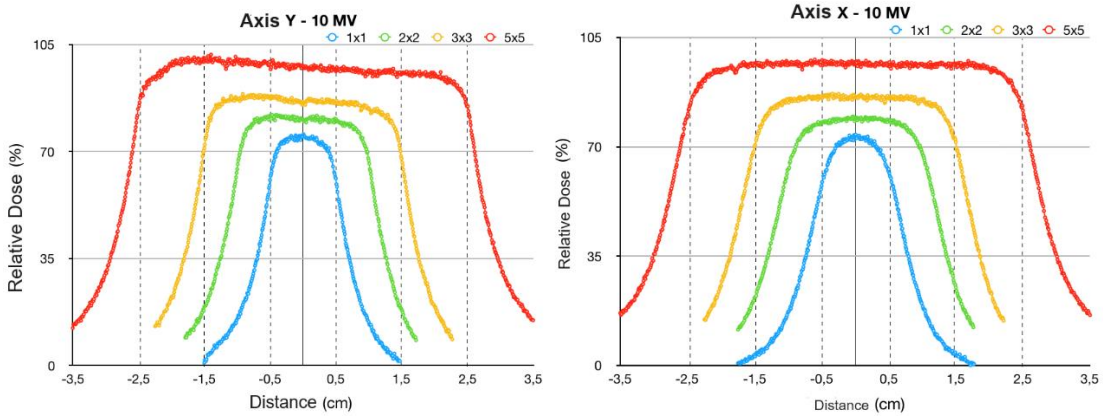

Fig. 6. The Figure presents the axial dose variation for the 10 MV beam of the film inside the solid water phantom.

For the 2x2 cm² and 3x3 cm² fields, there are differences in the relative dose, in which the latter reached a higher dose, presenting the smaller fields with a greater dose reduction when at a higher photon energy. The greatest distortion (fall) occurs in the 5x5 cm² field, but lower than it would be for the 6.0 MV voltage due to the higher energy of the photons at 10 MV. The axial dose profile at 1x1 cm² as an option for neurosurgery treatments using radiotherapy. Table 11 below presents the relative values of the Relative Dose for the large field of 5x5 cm², in which on the X and Y axes, there is a difference for the field of 5x5 cm², due to the greater bulging on the Y axis, due to the planning filter and for the small fields of 1x1, 2x2, 3x3 cm², indicating that the Relative Dose for the last two fields mentioned, between the X and Y axes of the fields mentioned, are close.

Tab. 3. Results in PDP Irradiation Fields in 10 MV.

Field Size (cm²)	**Relative Dose (%)**	**Axis X**	**Axis Y**
1x1	74.01±0,73	72,38±0,83	74,33±0,63
2x2	79,77±0,96	78,12±1,06	80,47±0,86
3x3	85,94±0,76	85,98±0,46	86,66±1,06
5x5	97,27±0,98	96,45±0,5	97,74±1,47

4. CONCLUSION

In this work, a solid water phantom was irradiated by a photom beam generated with a 10 MV voltage from a Linear Accelerator. The phantom was irradiated in four different field sizes, including small field sizes. The water phantom was irradiated with 3,0 Gy in the maximum dose value. Absorved dose measurements were performed using radiochromic film sheets inside the solid water phantom. These films recorded the profile of absorbed dose variations in depth and in a specific axial plane at 4 cm depth. It was observed variations in the behavior of the dose deposition in depth, where all the values of the small fields were smaller. As smaller was the field sizeraz, as smaller was the absorbed dose.

In the analysis of the large fields of 5x5 and 10x10 cm², for axial irradiation (transverse), the fields showed a decrease in the X-axis of irradiation, raising the doses above 100% in part of the axis. In the fields considered small, in axial irradiation, the 2x2 and 3x3 cm² fields had close relative doses. For the electrical voltage and energy of the photon beams at 10 MV, the relative doses for the small fields of 2x2 and 3x3 cm² have insignificant difference between them. The smaller the field, the higher the average energy of this beam when measurements are made on solid water simulating objects. This aspect is a characteristic pointed out of the three main points of the effects of Small Fields.

The irradiation of 10 MV in the accelerator A1 is like the irradiation of the shafts when using the electrical voltage (beam energy) of 6.0 MV. Noticeably, when the energy of the beams is raised to 10 MV, the drop in the X axis is greater than for 6.0 MV, in the large fields of 5x5 and 10x10 cm², showing that the fluence of the photons produced in the linear particle accelerator varies with the size of the field and the depth of the phantom object, the small fields in their lateral dimensions, causing the penumbras on both sides of the field to overlap, making the commonly used detectors too large in relation to the size of the radiation field, which can interfere with the dose distribution behavior.

ACKNOWLEDGMENT

This research was supported by Coordination for the Improvement of Higher Education Personnel (CAPES), National Council for Scientific and Technological Development (CNPq), National Nuclear Energy Commission (CNEN) and Minas Gerais Research Support Foundation (FAPEMIG). We thank to Mater Dei Hospital and Health Network who provided structure that greatly assisted the research. We would also like to show our gratitude to the Department of Nuclear Engineering for sharing their radiochromic film EBT3.

REFERENCES

[1] F. M. Khan, The physics of radiation therapy. 6th Edition, New York, Ed. Lippincott Williams & Wilkins (2010).

[2] A. P. Mourão and F. A. de Oliveira, Fundamentos de radiologia e imagem, 1ª Edição, Belo Horizonte, MG, Difusão Editora (2018).

[3] SCAFF, L. A. M, Física na radioterapia: a base analógica de uma era digital, 1ª Edição, São Paulo – SP, Editora Projeto Saber (2010).

[4] S. S. Ahmad, S. Duke, R. Jena, M. V. Williams, and N. G. Burnet, Advances in radiotherapy, Bmj: Leading Medical, Research, News, Education, Opinion, Vol. 345, pp. 1-19 (2012).

[5] R. G. L. Júnior, Avaliação das perturbações físicas de feixes de raios x em pequenos campos estáticos: Uma Abordagem Teórica pelo Método de Monte Carlo, Tese, Departamento de Engenharia Nuclear da Universidade Federal de Minas Gerais, Brasil (2018).

[6] B. Mijnheer, Clinical 3D dosimetry in modern radiation therapy. CRC Press, 2017. C.F. T. Portela and A.P. Mourão.: Preprint submitted to Elsevier Page 13 of 14. Dose Profile Evaluation for Small Fields.

[7] IAEA, "Technical report series no. 483 "dosimetry of small static fields used in external beam radiotherapy an international code of practice for reference and relative dose determination," 2017.

[8] R. G. Leão Jr, R. V. Sousa, A. H. Oliveira, H. L. L. Silva, and A. P. Mourão, "Validação de um modelo computacional de acelerador linear varian clinac 2100 utilizando o código egsnrc para utilização em dosimetria de pequenos campos.," Brazilian Journal of Radiation Sciences, vol. 6, no. 1, 2018.

[9] M. K. R. Nasir, N. Amjad, A. Razzaq, T. Siddique, Measurement and Analysis of PDDS Profile and Output Factors for Small Field sizes by cc13 and micro-chamber cc01, International Journal of Medical Physics, Clinical Engineering and Radiation Oncology, Vol. 6, pp. 36-56 (2017).

[10] F. Crop, N. Reynaert, G. Pittomvils, L. Paelinck, C. De Wagter, L. Vakaet, and H. Thierens, The influence of small field sizes, penumbra, spot size and measurement depth on perturbation factors for microionization chambers, Physics in Medicine & Biology, Vol. 54-69, pp. 2951 (2009).

[11] DAS, I. J.; DING, G. X.; AHNESJÖ, A, Small fields: nonequilibrium radiation dosimetry, Medical physics, Wiley Online Library, V. 35, pp. 206–215 (2008).

[12] Indra J Das, Paolo Francescon, Jean M Moran, Anders Ahnesjö, Maria M Aspradakis, Chee-Wai Cheng, George X Ding, John D Fenwick, M Saiful Huq, Mark Oldham, Chester S Reft, Otto A Sauer, Report of AAPM Task Group 155: Megavoltage Photon Beam Dosimetry in Small Fields and Non-equilibrium Conditions, Medical physics, Wiley Online Library, v. 48, pp. e886–e921 (2021).

[13] https://www.elekta.com/products/radiation-therapy/versa-hd/ acessado em 11 de setembro de 2024.

[14] G. Narayanasamy, D. Saenz, W. Cruz, C. S. Ha, N. Papanikolaou, S. Stathakis Commissioning an elekta versa hd linear accelerator, Journal of applied clinical medical physics, Wiley Online Library, V. 17, pp. 179–191 (2016).

[15] R. Hill, Z. Kuncic, C. Baldock, The water equivalence of solid phantoms for low energy photon beams. Medical physics, Wiley Online Library, V. 37, pp. 4355–4363 (2010).

[16] M. A. Gargett, A. R. Briggs, J. T. Booth, Water equivalence of a solid Phantom material for radiation dosimetry applications, Physics and Imaging in Radiation Oncology, Elsevier, V. 14, pp. 43–47 (2020).

[17] S. Aldelaijan, S. Devic, Comparison of dose response functions for EBT3 Model Gafchromic™ Film Dosimetry System, Physica Medica, Elsevier, v. 49, pp. 112–118 (2018).

[18] DEVIC, S. Radiochromic film dosimetry: past, present, and future. Physica Medica, Elsevier, V. 27, pp. 122–134 (2011).

[19] Marina Fuss, Eva Sturtewagen, Carlos De Wagter, Dietmar Georg, Dosimetric Characterization of Gafchromic EBT Film and its Implication on Film Dosimetry Quality Assurance, Physics in Medicine & Biology, V. 52, pp. 4211-25 (2007).

[20] J. Luvizotto, Caracterização do filme radiocrômico Gafchromictm modelo EBT3 para uso em braquiterapia, Dissertação, Instituto de Pesquisas Energéticas e Nucleares – IPEN, Comissão Nacional de Energia Nuclear - CNEN (2015).

[21] https://www.ashland.com/industries/medical/radiotherapy-films/ebt3 acessado em 11 de setembro de 2024.

[22] Technical Report Series no. 483 - Dosimetry of Small Static Fields used in External Beam Radiotherapy - An International Code of Practice for Reference and Relative Dose Determination, “TRS nº 483”, IAEA – International Atomic Energy Agency, CH (2017).

[23] S. Lam, D. Bradley, M. U. Khandaker, Small-Field Radiotherapy Photon Beam Output Evaluation: Detectors Reviewed, Radiation Physics and Chemistry, Elsevier, v. 178, pp. 108950-108960 (2021).

[24] T. C. Zhu, Small field: dosimetry in electron disequilibrium region, Journal of Physics: Conference Series, V. 250, pp. 012056-012067 (2010).